

Original Article

The Chinese medicine, Jianpi Huayu Decoction, inhibits the epithelial mesenchymal transition via the regulation of the Smad3/Smad7 cascade

Chong Zhong^{1*}, Yong-Fa Zhang^{2,3,4*}, Jun-Hai Huang¹, Zi-Yu Wang¹, Qiu-Yuan Chen¹, Li-Tian Su¹, Zhen-Tao Liu¹, Cheng-Ming Xiong¹, Zhi Tao¹, Rong-Ping Guo²

¹Department of Hepatobiliary Surgery, The First Affiliated Hospital of Guangzhou University of Chinese Medicine, Guangzhou 510405, China; ²Department of Hepatobiliary Oncology, Cancer Center of Sun Yat-sen University, Guangzhou 510060, China; ³Department of Liver Surgery, Fudan University Shanghai Cancer Center, Shanghai, China; ⁴Department of Oncology, Shanghai Medical College, Fudan University, Shanghai, China. *Co-first authors.

Received January 14, 2017; Accepted April 30, 2017; Epub June 15, 2017; Published June 30, 2017

Abstract: Background: Hepatocellular carcinoma (HCC) is one of the most common and aggressive malignant tumors in the world. In China, traditional medicine is commonly used in the treatment of cancer. Among these medicines, Jianpi Huayu Decoction (JHD) is a typical clinical prescription against multiple tumors. However, the exact function and targets of JHD are currently unknown. The aim of this study is to assess the efficacy of JHD against HCC. Methods and results: Hepatic carcinoma SMMC7221 cells were treated with JHD drug-serum in a dose- and time-dependent manner. Real-time PCR (RT-PCR), western-blot (WB), and immunofluorescence microscopy revealed that JHD increased both the mRNA and protein levels of Smad7 and decreased the protein level of p-Smad3. It subsequently increased the E-cadherin expression level and decreased those of N-cadherin and Vimentin. Metastasis and invasion were eventually inhibited, as determined by the wound healing and transwell invasion assays. Treatment of Tanshinone IIA (Tan IIA) showed similar results as JHD, indicating that it is most likely the main functional drug monomer of JHD. The *in vivo* assay in nude mice also revealed the efficacy of JHD to inhibit epithelial mesenchymal transition (EMT). Conclusion: JHD was shown to be an effective therapeutic strategy against HCC.

Keywords: Hepatocellular carcinoma, traditional Chinese medicine, Jianpi Huayu Decoction, Tanshinone IIA, epithelial mesenchymal transition

Introduction

Liver cancer is currently the second leading cause of cancer-related death worldwide, with more than 850,000 new cases in 2012, and the figure is on the rise [1]. Furthermore, liver cancer is the fourth most commonly diagnosed cancer in China, with an incidence of 466,100 new cases and a mortality of 422,100 deaths in 2015 [2]. Hepatocellular carcinoma (HCC) accounts for around 90% of primary liver cancers and is strongly linked to cirrhosis and infection with hepatitis B virus (HBV) or hepatitis C virus (HCV) [3]. Although the incidence of liver cancer and mortality have been decreasing in China due to the control of early childhood infections, it is too early to have made an impact for all ages [2]. Because suitable surgical procedures are limited and the survival rate is strongly dependent on the stage of the tumor,

the presence of vascular invasion, and micro-metastases, the prognosis for HCC is still typically poor [4]. The underlying mechanisms of cancer invasion are still unknown, but the epithelial mesenchymal transition (EMT) is expected to trigger the invasive properties of tumors [5].

EMT is a complicated process during embryonic development and in cancer [6], but may be an important step leading to invasion and metastasis [7]. At the molecular level, EMT is characterized by loss of epithelial cell markers, including the cell adhesion protein, E-cadherin, and by the acquisition of mesenchymal markers, such as Vimentin [8, 9]. In ovarian and breast cancer, it usually increases the expression of Snail and decreases E-cadherin expression [10]. Transforming growth factor β 1 (TGF- β 1) has been shown to induce EMT via Snail in different cell types,

including hepatocytes, but the underlying mechanisms are poorly understood [11, 12].

Multiple chemotherapeutic drugs are widely used to treat HCC, but their side effects hamper their clinical application and efficacy [13]. Compared with chemotherapeutic drugs, natural products have relatively fewer side effects and have also been shown to possess beneficial therapeutic effects against cancer [14-16]. According to the precepts of traditional Chinese medicine, the intended effect includes not only alleviation of symptoms, but also the restoration and maintenance of the body's homeostasis [17]. It is, therefore, similar to modern multi-targeted therapeutics. The traditional Chinese herbal formula, Jianpi Huayu Decoction (JHD), has been widely used to treat cancer in a clinical setting [18]. It can suppress the growth of many types of cancer both *in vivo* and *in vitro* [18]. However, the exact mechanisms, including its functions and targets, are currently unknown.

In order to further elucidate the mechanisms behind the tumoricidal activity of JHD, we used hepatic cancerous cells and nude mice to investigate its anti-proliferative activity against HCC. In addition, we attempted to verify the correlation between JHD and EMT, in order to determine its exact functions and targets.

Materials and methods

Preparation of the JHD extract

The herbs for the JHD extract were as follows: 20 g Panax ginseng, 15 g Atractylodes macrocephala Koidz, 12 g Dioscorea opposita thumb, 15 g Wolfiporia extens, 10 g Cortex Moutan Radicis, 15 g Salvia miltiorrhiza bunge, 10 g Curcuma aromatica, 10 g curcuma phaeocaulis val, 15 g Radix Bupleuri, and 6 g Radix liquiritiae. The total weight of the dried herbs was 128 g. The herbs were blended into double-distilled water for 1 h and then heated at 100°C for 2 h, after which the residue was boiled for 2 h with distilled water. The extracts were subsequently diluted to 1 g herb/ml and filtered with a 0.2 µm filter. The extract was stored at -20°C until use.

Cell culture and treatment

Both SMMC7721 and MHCC-97L cells (ATCC, USA) were grown in DMEM-H medium, which was supplemented with 10% fetal bovine serum

and 1% penicillin/streptomycin, and kept in a 5% CO₂, 37°C humidified incubator. The medium was routinely changed every 2 or 3 days. Cells were cultured, amplified, and passaged and after 3 days, were digested and centrifuged. Cell morphology was viewed under a light microscope and suspended to a final concentration of 1×10⁶/ml.

The suspensions of SMMC7221 or MHCC-97L cells (1×10⁶/ml) were seeded onto 24-well plates for a 24-h incubation at 37°C. The culture medium was then changed. The cells were exposed to drug-serum or different reagents, according to the specific experiment (see results). The TGF-β1 solution was diluted at 20 µM and was purchased from Sigma-Aldrich, USA. Tanshinone IIA (Tan IIA), Rh2, and Rg3 were purchased from Aladdin (Shanghai, China).

Wound healing assay

The SMMC7221 or MHCC-97L cell suspensions (1×10⁶/ml) were seeded onto 24-well plates with barriers. After a 24-h incubation at 37°C, the barriers in each well were removed. The wounds were observed and their width determined using microscopy. The cells were then incubated for 48 h under corresponding treatment and were then observed and the wound width was measured every 24 h

Transwell invasion

24-well plates with Matrigel invasion chambers (Corning, USA) were used according to the manufacturer's protocol. The top chambers were seeded with a 200 µl diluted suspension of SMMC7221 or MHCC-97L cells (5×10⁴ cells), and the bottom chambers were filled with 500 µl culture medium containing 20% FBS. After 24 h of incubation, cells that migrated through the membrane were fixed with methanol and stained with 0.1% crystal violet (w/v). The stained cells were detected using optical microscopy.

Immunofluorescence microscopy

Cells were diluted at 5×10⁴ cells/ml and seeded in 48-well plates with 200 µl per well. They were then incubated overnight under corresponding treatment. The culture medium was removed, and the cells were washed three times with PBS, were fixed, permeabilized,

blocked, and incubated with primary antibody. After three washes with PBS, IgG antibody coupled with FITC was added and cells were subsequently incubated for 1 h at room temperature. The cells were again washed with PBS three times and then stained with 5 µg/ml DAPI for 3 min. They were once again washed with PBS and blocked. Images were obtained with microscopy. The primary antibodies, including anti-E-cadherin, anti-Vimentin, and anti-N-cadherin, were purchased from ABCam.

Smad3 overexpression and Smad7 suppression assay

The Smad3 overexpression vector, LV-Smad3, and the Smad7 suppression short hairpin RNA (shRNA), LV-shSmad7, were designed and packaged into a lentivirus by Forevergen biotechnology, Guangzhou, China. The MHCC-97L cells (1×10^6 /ml) were seeded into 24-well plates overnight at 37°C. The lentivirus was thawed in a 37°C water bath and diluted in DMEM medium. The medium from the cultured cells was then removed and added into the lentivirus solution. Polybrene was added and gently mixed with a pipette several times. The cells were incubated overnight at 37°C, the lentiviral culture medium was removed, and it was changed with fresh culture medium. The cells were cultured for 10-12 days. Fluorescence microscopy was used in order to observe and screen the cells with positive expression. Those cells were then collected for the downstream applications.

Animal experiment

Fifteen Wistar rats (Vitalriver, Beijing, China) weighing 250 ± 20 g were used for the drug assay. The rats were assigned to three groups: (1) control, (2) low concentration of JHD extract, and (3) high concentration of JHD extract. The original JHD extract in 1 g herb/ml was treated as the high concentration, while the low concentration was diluted 2 times from the original extract. The JHD extract was given by gavage at a 5 ml/dose/kg, twice per day. The animals in the control group were treated with same volume of saline. After 7 days of treatment, the rats were anesthetized and whole blood was extracted from the abdominal arteries. The whole blood was subsequently centrifuged in order to isolate the serum.

The animal studies were approved by a committee from The Institute for the Research of Medical Ethics of Guangzhou University of Chinese Medicine. The 6-8 week old nude mice were anesthetized by injecting chloral hydrate at a dose of 45 mg/kg weight. The mice were separated into two groups for SMMC7221 cell injection, namely the control group and the JHD treatment group, with 10 animals in each. The nude mice were also assigned for MHCC-97L cell injection and separated into three groups with 10 animals in each group. These were Sh-Control+vehicle, Sh-Smad7+vehicle, and Sh-Smad7+herbal medicine (HM). Under sterile conditions, the mice were fixed face down on a surgical table and the skin was partially shaved, preserved, and sterilized. A 5 mm abdominal incision was made at the left flank, between the midaxillary line and the posterior axillary line to expose the spleen. Suspensions (100 µl) of SMMC7221 cells (1×10^6 /ml) and Sh-Smad7 and Sh-Control transfected MHCC-97L cells (1×10^6 /ml) were injected into lower pole of the spleen. The spleen was then returned to the peritoneal cavity and the abdominal wall was closed. Two days after injection, the nude mice in the JHD treatment group were given a 0.5 ml JHD extract by gavage once a day at 1 g herb/ml. Meanwhile, the control group mice were treated with same volume of saline. All mice were then observed for survival and tumor formation. After 5 weeks of treatment, the mice were sacrificed, and the cancerous tissues were removed by sterile surgery and were placed in RNase-free saline. The weight and size of the cancerous tissues were then examined, fixed by formalin, and embedded in paraffin.

Hematoxylin-eosin (HE) staining

The formalin-fixed and paraffin-embedded tissue was cut into sections and placed on the slides. The slides were deparaffinated with xylene and washed with ethanol and water. Next, the slides were stained with hematoxylin and rinsed with water for 10 minutes and ethanol for 5 s. The slides were then stained with eosin and incubated for 10 s. After incubation, the slides were washed with water and cover-slipped. The slide images were obtained by microscopy.

Immunohistochemical staining

The tissue was then deparaffinated and washed twice with PBS before being blocked with 3%

Table 1. The primer details in this study

Gene symbol	Sequences
Smad7	5'-GGGGCTTTCAGATTCCCAAC-3'(f) 5'-CAAAAGCCATTCCCCTGAGG-3'(r)
SMAD3	5'-TGCTCTAGAATGTCGTCCATCCTGCCTT-3'(f) 5'-ATTGCGGCCGCCTAAGACACACTGGAACAGCGG-3'(r)
Snail	5'-CTTCCAGCAGCCCTACGAC-3'(f) 5'-CGGTGGGGTTGAGGATCT-3'(r)
Zeb1	5'-CTGATTCCCCAGGTGGCATA-3'(f) 5'-GGGCGGTGTAGAATCAGAGT-3'(r)
Zeb2	5'-ACTCTGTCTGTCTCGCAA-3'(f) 5'-GCTCGATAAGGTGGTGCTTG-3'(r)
GAPDH	5'-AGGTCCACCACTGACACGTT-3'(f) 5'-GCCTCAAGATCATCAGCAAT-3'(r)

H₂O₂ for 5-20 min and washed, again, three times with PBS. The tissue was fixed by water incubation at 95°C and then washed with PBS. The tissue was then blocked with 5% BSA and incubated with primary antibody at 4°C overnight. After three more washes, the tissue was incubated with secondary antibody for 1 h at room temperature. After a complete wash in PBS, the sections were developed in a freshly prepared diaminobenzidine solution (DAB), then counterstained with hematoxylin, dehydrated with graded ethanol, cleared with xylene, and cover-slipped. The expression levels of the molecules were estimated by microscopy.

Western blot analysis

The protein was purified from SMMC7721 or MHCC-97L cells. Protein concentrations were determined with the BCATM-Protein Assay Kit (Fulengen, Guangzhou, China). Ten µl of protein was subjected to 10% SDS-PAGE and was then transferred onto nitrocellulose membranes. The membranes were blocked with 5% nonfat milk in phosphate-buffered saline containing 0.1% Tween 20 for 1 h at room temperature and incubated overnight at 4°C with the primary antibody. After three washes, membranes were incubated in blocking buffer with a secondary antibody coupled to horseradish peroxidase for 2 h at room temperature. The complexes were then detected with ECL (Forevergen, Guangzhou, China). Anti-Smad7, anti-Smad3, anti-Snail, anti-E-cadherin, anti-EpCAM, anti-Vimentin, anti-N-cadherin, and anti-GAPDH were obtained from ABCam.

Real-time PCR assay

Total RNA was prepared using TRIzol (Invitrogen, Paisley, Scotland) following the manufacturer's. Genomic DNA-free RNA was then converted into cDNA using M-MLV Reverse Transcriptase (Promega, Melbourne, Australia) and PCR amplification was performed using GoTaq qPCR Master Mix (Promega, Melbourne, Australia) on CFX96 (Bio-Rad, CA). The specific primer is shown in **Table 1**.

Statistical analysis

Comparisons were performed using independent t-tests with SPSS software. Data are reported as mean ± standard deviation (S.D.). Analyses of multiple groups were assessed using one way ANOVA followed by Tukey's post-hoc test. The significance was established as P < 0.05.

Results

JHD treatment inhibits EMT and thus cell migration and invasion

For the purpose of estimating the efficacy of JHD treatment by its inhibition of EMT, the expressions of related genes were measured. Therefore, SMMC7221 cells were treated with a low concentration of drug serum for 72 h. The gene expressions were measured accordingly every 12 h. The mRNA and protein expression of the genes was measured by qPCR and western blot and results showed that the level of Smad7 mRNA was increased by ~2.5-fold and that of Snail was decreased by ~0.5-fold after 48 h and 72 h of drug-serum treatment (**Figure 1A**). However, the Smad3 mRNA level showed no difference at any time interval. Thus, we evaluated the protein expressions of p-Smad3, Smad3, and also Snail. The protein expression of Snail was consistent with the mRNA expression; it began to significantly decrease at 48 and 72 h. However, the protein expression of p-Smad3 was downregulated at 48 h and 72 h, although the protein expression of Smad3 hardly showed a difference at any interval (**Figure 1C** and **1D**). This indicates that the drug-serum was more efficient in reducing the phosphorylation of Smad3 than in regulating its expression. According to the above results, the

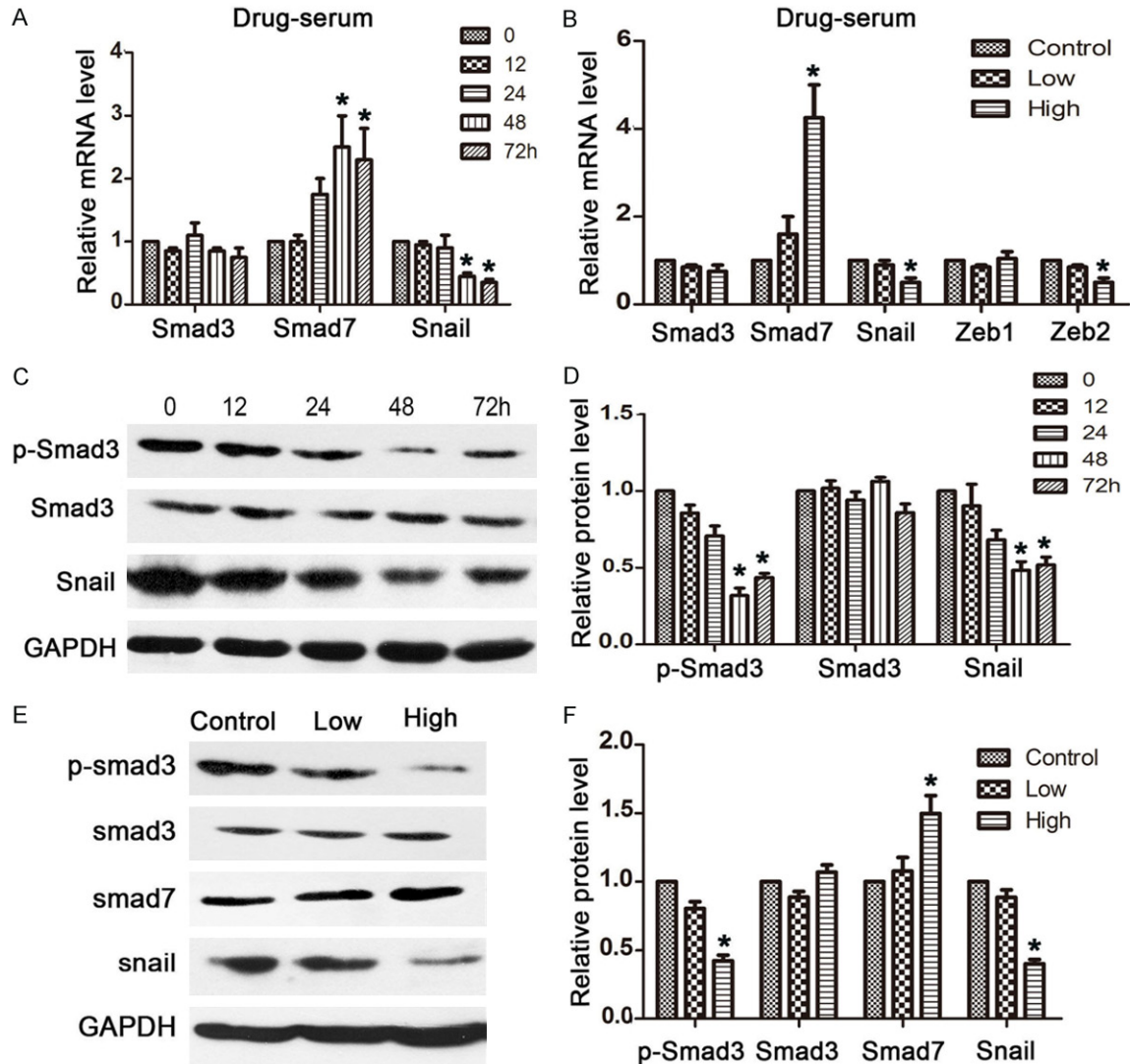


Figure 1. JHD regulates the expression level of the Smad3/Smad7 cascade in SMMC7221 cells. A: The mRNA expression levels of cancer related genes after SMMC7221 cells were treated with JHD drug-serum for 0, 12, 24, 48, and 72 h; B: The mRNA expression levels of cancer related genes after SMMC7221 cells were treated with low- and high-concentration of JHD drug-serum. C and D: Western blot results for the protein expression levels of cancer related genes after SMMC7221 cells were treated with JHD drug-serum for 0, 12, 24, 48, and 72 h; E and F: Western blot results for the protein expression levels of cancer related genes after SMMC7221 cells were treated with low- and high-concentration of JHD drug-serum. p-Smad3: phosphorylated Smad3. * $P < 0.05$.

drug-serum reached its best performance at 48 h. Therefore, we conducted a comparison of the gene expressions in SMMC7221 cells under either low or high concentrations of drug-serum for 48 h. The high-concentration induced more significant changes than the low-concentration. In this case, the mRNA level of Smad7 obtained around a 2-fold higher increase and Snail was shown to decrease even further (Figure 1B). We also tested the mRNA expressions of the relevant genes, Zeb1 and Zeb2, but only the expression of Zeb2 decreased to 50%

under high-concentration treatment. The protein level also showed consistent results that Smad7 increased and p-Smad3 and Snail decreased most significantly under high-concentration treatment (Figure 1E and 1F).

The protein expression of the critical factors, E-cadherin and N-cadherin, which affect EMT, was subsequently determined. Treatment promoted the expression of E-cadherin but suppressed the expression of N-cadherin. In particular, E-cadherin showed a positive relation-

Jianpi Huayu Decoction inhibits EMT

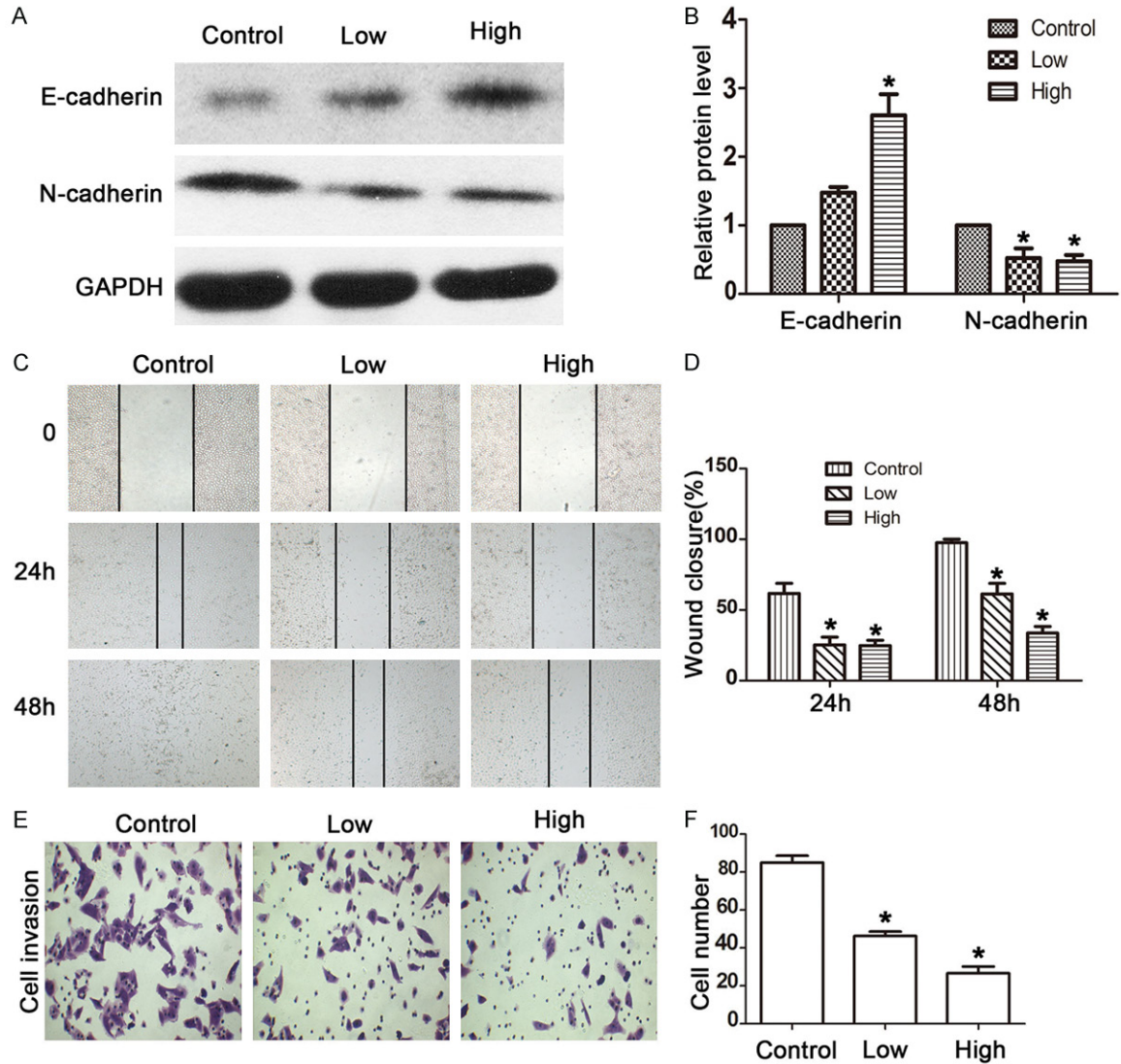


Figure 2. JHD inhibited the EMT of SMMC7221 cells. A and B: JHD drug serum increased the protein expression of E-cadherin and decreased the protein expression of N-cadherin; C and D: Wound healing assay to assess the cell migration of SMMC7221 cells treated with JHD drug-serum; E and F: Transwell assay to assess the cell invasion of SMMC7221 cells treated with JHD drug-serum. * $P < 0.05$.

ship with increasing concentrations of drug-serum (Figure 2A and 2B). Wound healing and transwell invasion assays were performed to detect cell migration and invasion. Compared with the control group, the treatment group presented with efficient inhibition of both cell migration (Figure 2C and 2D) and invasion (Figure 2E and 2F). In addition, the high-concentration of drug-serum was more efficient in decreasing wound closure and the number of invasive cells. These findings suggest that JHD extract inhibits EMT by inducing increased expression of Smad7 and decreased expression of p-Smad3 and Snail in mRNA and/or protein expression, subsequently leading to higher

E-cadherin but lower N-cadherin expression, and therefore inhibiting cell migration and invasion.

Tan IIA is the critical drug monomer regulating Smad3 and Smad7 expression

Since the JHD extract components are complicated, in order to understand the exact component that inhibits EMT, we treated SMMC7221 cells with Ginsenoside (Rh2 and Rg3), Atractylenolide I (ATL-I), and Tan IIA, which are constituents of the JHD extract. Smad7 was selected to be a reference marker to evaluate the efficacy of the above monomers. Western blot

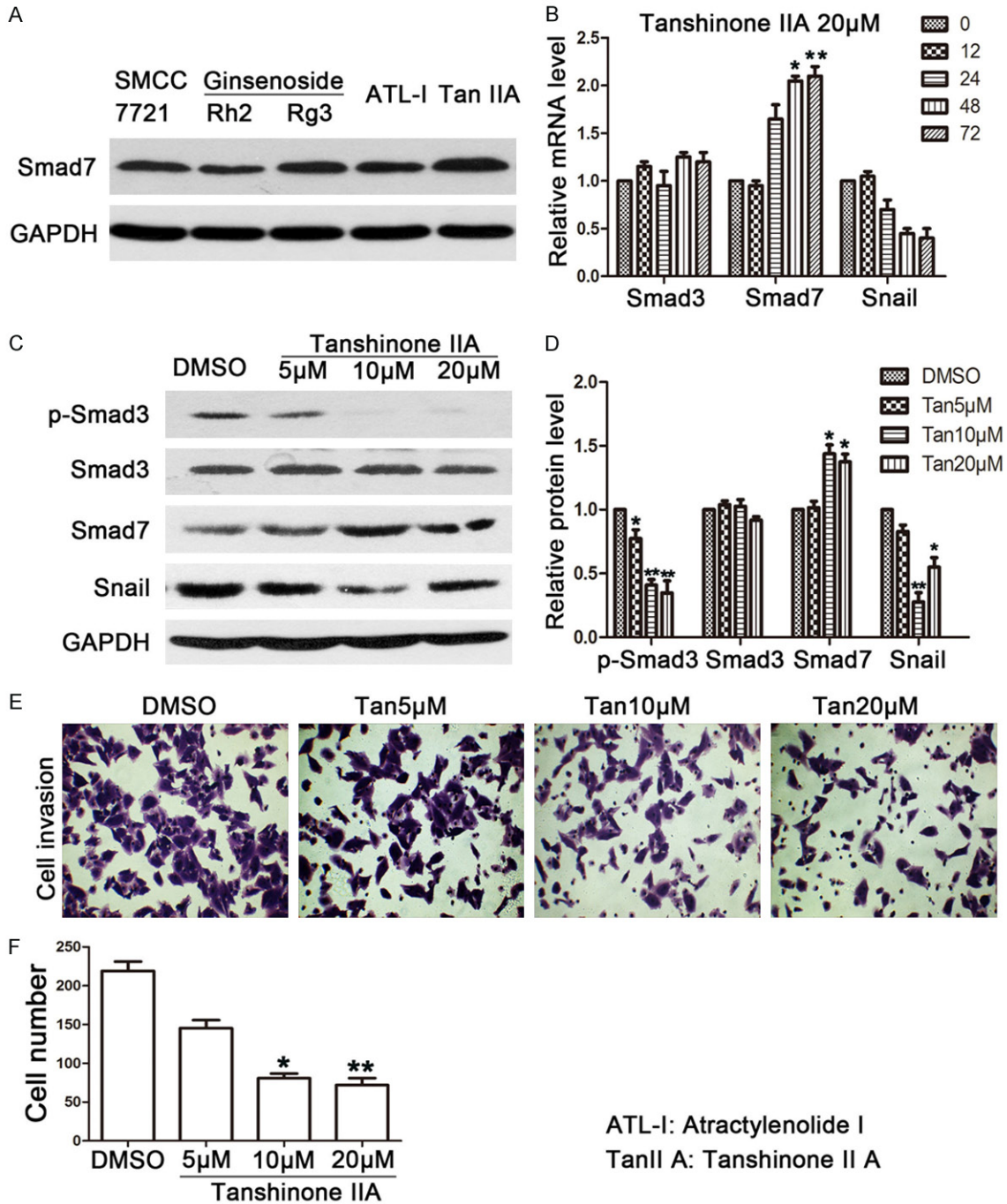


Figure 3. JHD functional drug monomer screening. A: The western blot results of Smad7 when SMMC7221 cells were treated with 50 μ M Rh2 and Rg3, 100 μ M ATR, and 20 μ M Tan IIA; B: The expression levels of Smad7 and Snail showed a time-dependent manner when SMMC7221 cells were treated with 20 μ M Tan IIA; C and D: The expression levels of p-Smad3, Smad3, Smad7, and Snail when SMMC7221 cells were treated with Tan IIA in different concentrations; E and F: Cell invasion level when SMMC7221 cells were treated with Tan IIA. *compared with 0 h group or DMSO control group, $P < 0.05$; **compared with 0 h group or DMSO control group, $P < 0.01$. ATL-1: Atractylenolide I, Tan IIA: Tanshinone IIA, p-Smad3: phosphorylated Smad3.

was carried out in order to measure Smad7 protein expression. According to the results, out of all of the monomers, Tan IIA obviously promoted Smad7 (Figure 3A). We then verified its effi-

cacy and exact functions. The results were consistent with those of treatment with whole JHD extract, in that the mRNA levels of Smad7 and Snail increased and decreased, respectively, at

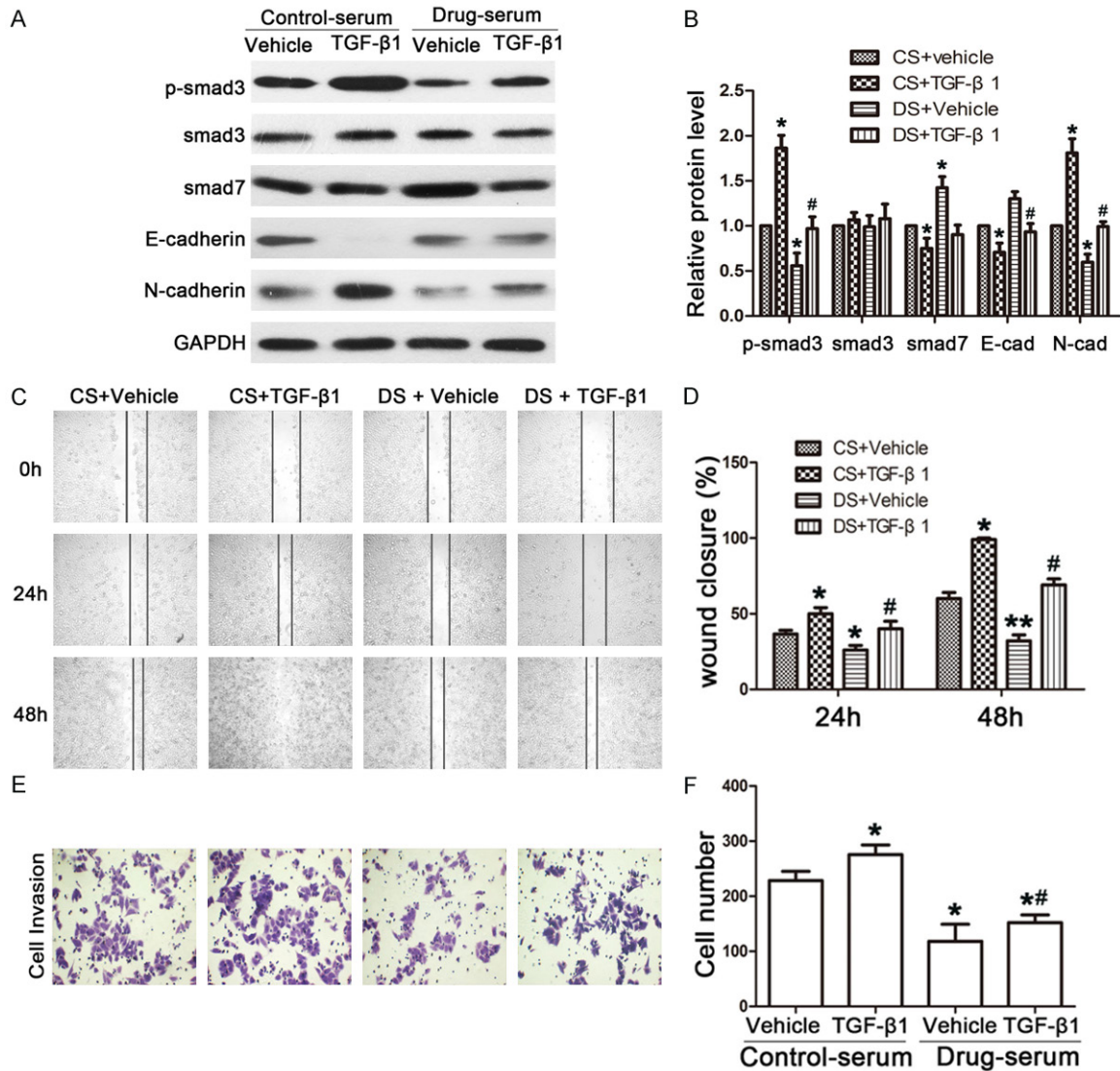


Figure 4. JHD regulated Smad3/Smad7 with TGF-β1 treatment. A and B: TGF-β1 solution adjusted EMT related gene expressions, but JHD drug-serum suppressed the function of TGF-β1; C and D: The wound healing assay assessed the cell migration level when SMMC7221 cells were treated with a TGF-β1 solution and drug-serum; E and F: The transwell invasion assay assessed the cell invasion level when SMMC7221 cells were treated with TGF-β1 solution and drug-serum. *compared with cs+vehicle group, $P < 0.05$; #compared with cs+TGF-β1 group, $P < 0.05$. CS: Control serum, DS: Drug serum.

48 and 72 h (Figure 3B). The concentration-related tendency was also seen in the protein levels of both p-Smad3 and Smad7, namely that a higher concentration led to more significant change (Figure 3C and 3D). There was, however, one exception. A dose of 20 μM Tan IIA decreased the protein level of Snail, but less significantly than a 10 μM dose. In this case, cell invasion was inhibited by Tan IIA so that the percentage of remaining invasive cells was 30% in both the 10 and 20 μM Tan IIA treatment groups, compared with the control group (Figure 3E and 3F).

JHD treatment mainly functions through the Smad3/Smad7 cascade

The expression of phosphorylated Smad3 (p-Smad3) and Smad7 presented consistent and constant expression patterns in both the drug-serum and Tan IIA treatments. Therefore, we assume that JHD treatment performs its functions mainly via the Smad3/Smad7 cascade. In order to further verify this assumption, we used TGF-β1 as an agonist to activate the cascade in SMMC7221 cells. At the same time, drug-serum was used to verify the exact func-

Jianpi Huayu Decoction inhibits EMT

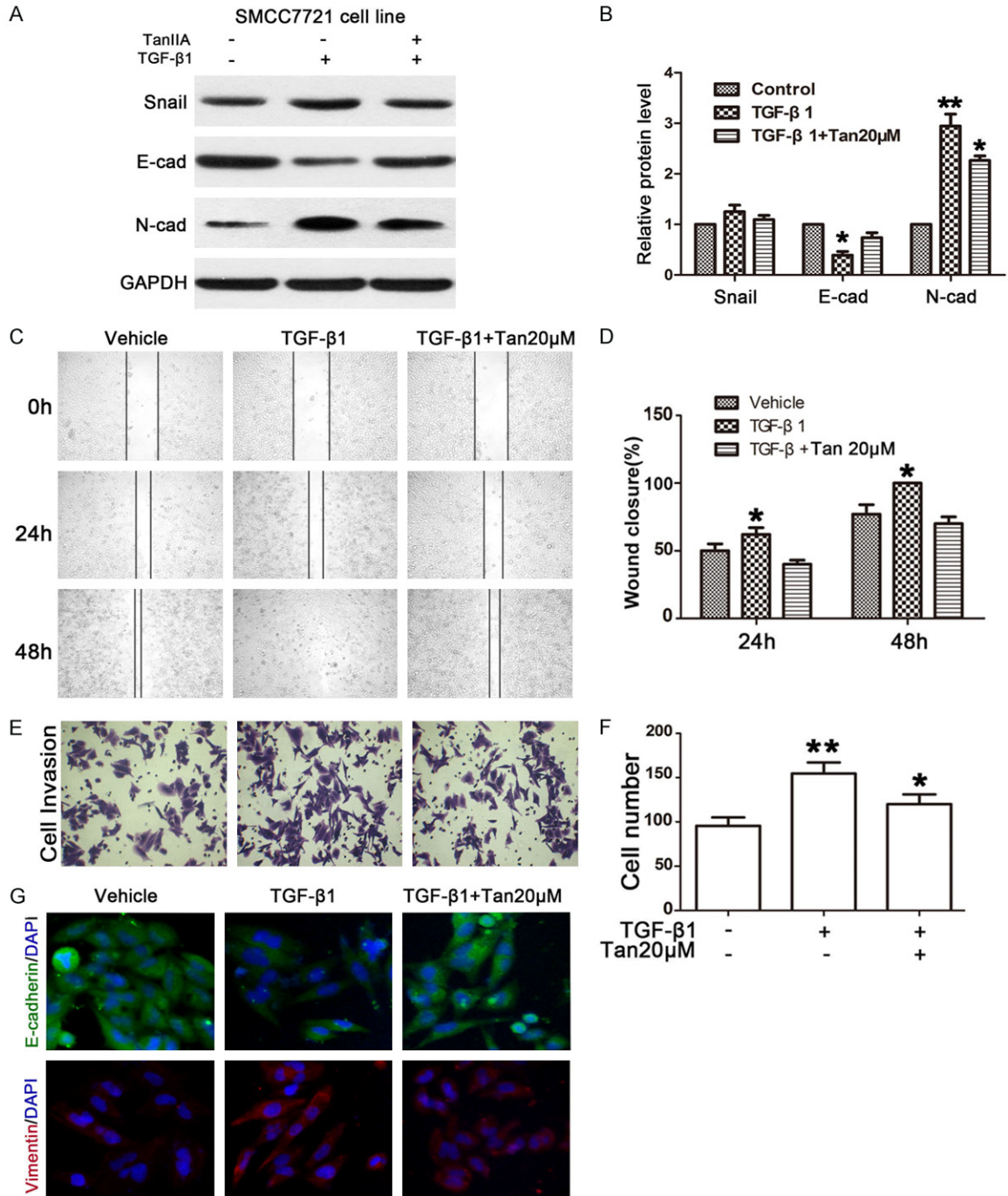


Figure 5. Tan IIA inhibited EMT in SMMC7221 cells. A and B: TGF-β1 solution adjusted EMT related gene expression but Tan IIA suppressed the function of TGF-β1; C and D: The wound healing assay assessed cell migration when SMMC7221 cells were treated with a TGF-β1 solution and Tan IIA; E and F: The transwell invasion assay assessed the cell invasion level when SMMC7221 cells were treated with a TGF-β1 solution and Tan IIA; G: Immunofluorescence microscopy determined the expression levels of E-cadherin and Vimentin in SMMC7221 treated with TGF-β1 solution and Tan IIA. *compared with control group, $P < 0.05$; **compared with control group, $P < 0.01$. E-cad: E-cadherin, N-cad: N-cadherin.

tions of JHD treatment. TGF-β1 was shown to be responsible for upregulating the expression of p-Smad3 and attenuating that of Smad7 (Figure 4A and 4B). This subsequently led to

the enhanced cell migration indicated by the increased wound closure (Figure 4C and 4D). In addition, cell invasion became more active and more invasive cells were therefore detected by

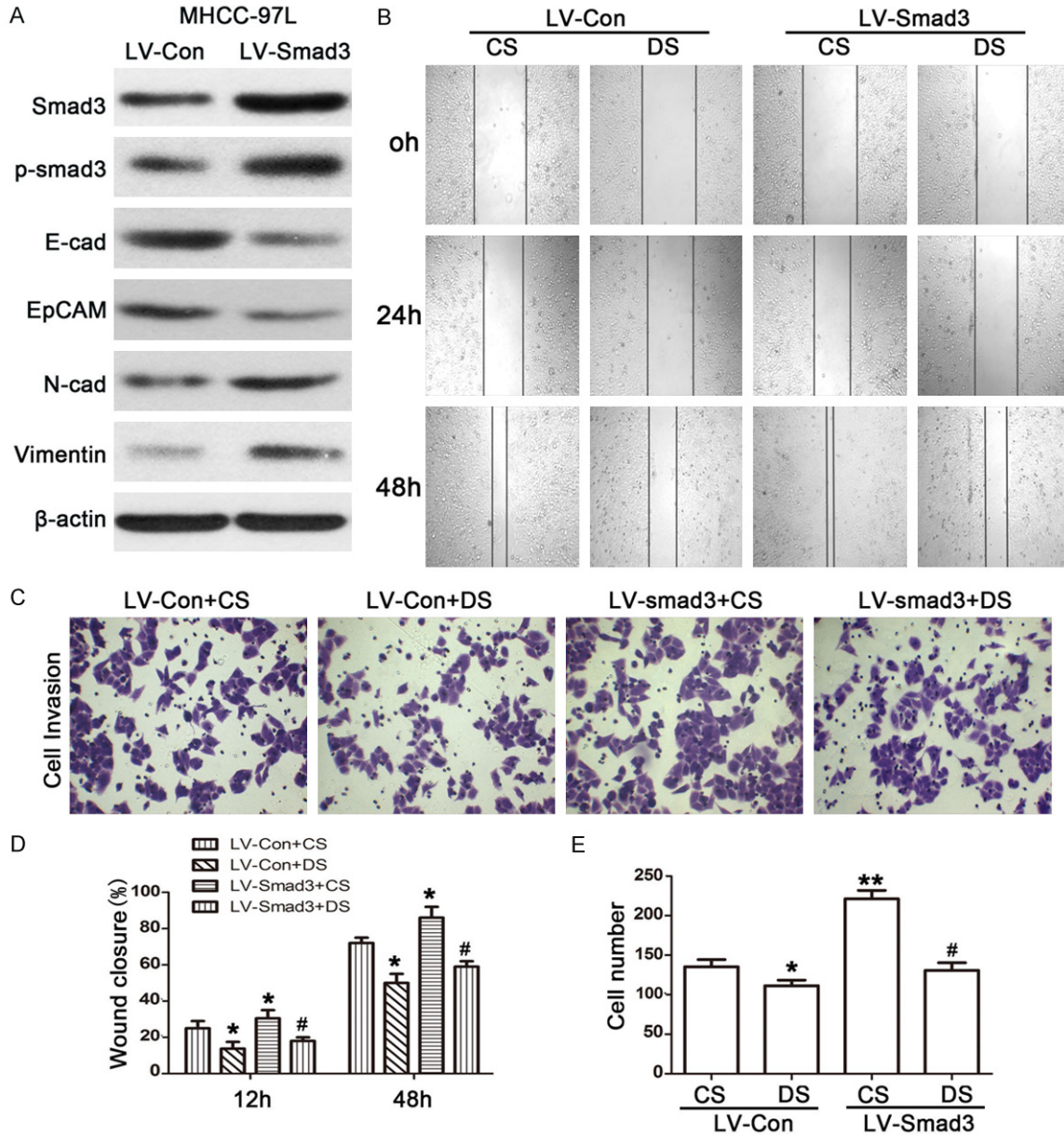


Figure 6. JHD drug-serum inhibited EMT when Smad3 was overexpressed in MHCC-97L cells. A: The protein expression levels of EMT related genes when Smad3 was overexpressed; B and D: The wound healing assay assessed cell migration when Smad3 was overexpressed in MHCC-97L cells; C and E: The transwell invasion assay assessed cell invasion when Smad3 was overexpressed in MHCC-97L cells. *compared with the cs+LV-Con group, $P < 0.05$; **compared with the cs+LV-Con group, $P < 0.01$; #compared with the cs+LV-Smad3 group, $P < 0.05$. CS: Control serum, DS: Drug serum.

the transwell invasion assay (Figure 4E and 4F). We then repeated a similar experiment using drug-serum instead of the regular serum to treat the SMMC7221 cells with and without TGF- β 1. Under these conditions, TGF- β 1 was observed to perform the same function of regulating the expressions of p-Smad3 and Smad7. Nevertheless, the drug-serum performed an opposite function that suppressed the expression of p-Smad3 while significantly increasing

the expression of Smad7 (Figure 4A and 4B). Consequently, cell migration (Figure 4C and 4D) and invasion (Figure 4E and 4F) were both suppressed, regardless of the presence of TGF- β 1. Therefore, these results prove that the drug-serum targets Smad3 and Smad7 but has no relationship with TGF- β 1. The regulation of the Smad3/Smad7 cascade is most likely a crucial step in the inhibition of hepatic cell EMT.

Jianpi Huayu Decoction inhibits EMT

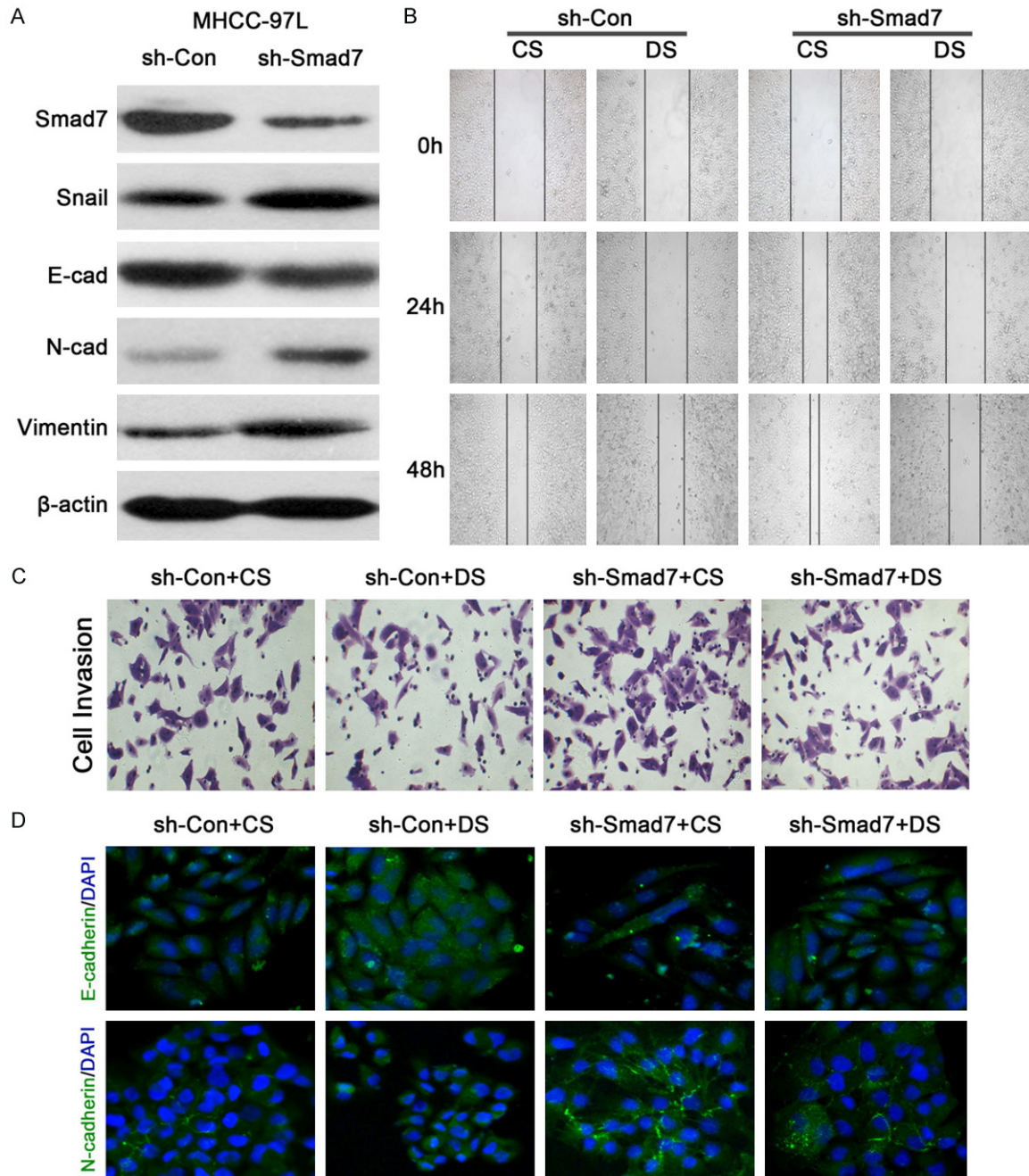


Figure 7. JHD drug-serum inhibited EMT when Smad7 was suppressed in MHCC-97L cells. **A:** The protein expression levels of EMT related genes when Smad7 was suppressed; **B:** The wound healing assay assessed cell migration when Smad7 was suppressed in MHCC-97L cells; **C:** The transwell invasion assay assessed cell invasion when Smad7 was suppressed in MHCC-97L cells; **D:** Immunofluorescence microscopy determined the expression levels of E-cadherin and N-cadherin when Smad7 was suppressed in MHCC-97L cells. CS: Control serum, DS: Drug serum, E-cad: E-cadherin, N-cad: N-cadherin, Con: Control.

Tan IIA inhibits the EMT of SMMC7221 cells

JHD and Tan IIA both perform functions in regulating the Smad3/Smad7 cascade, resulting in the inhibition of cell migration and invasion in SMMC7221 cells. We further verified the EMT

when SMMC7221 cells were treated with Tan IIA. This experiment was set up using TGF-β1 and Tan IIA to activate or suppress the Smad3/Smad7 cascade. The western blot results clearly showed that the key molecules in EMT, E-cadherin and N-cadherin, were significantly

affected by TGF- β 1 and Tan IIA treatment (**Figure 5A** and **5B**). When treated with TGF- β 1 only, the protein level of E-cadherin decreased, while the N-cadherin level increased, compared with the control group ($P < 0.05$). When the cells were treated with 20 μ M TGF- β 1 plus Tan IIA, the effect of TGF- β 1 was reversed, in that E-cadherin expression was upregulated and N-cadherin expression was downregulated compared with cells treated with TGF- β 1 alone. In this case, both cell migration and invasion were enhanced by treatment with TGF- β 1 but were attenuated by treatment with Tan IIA (**Figure 5C-F**). We then conducted immunofluorescence microscopy to observe the EMT level according to E-cadherin and Vimentin levels. The images showed that E-cadherin was stained green and Vimentin was stained red (**Figure 5G**). In the control group, E-cadherin was detected at a significant level but Vimentin was hardly detected at all. TGF- β 1 significantly activated EMT and thus E-cadherin was almost undetectable and Vimentin became obviously detectable. However, after adding Tan IIA, E-cadherin recovered to a level similar to that seen in the control group and Vimentin became undetectable. These results indicate that Tan IIA is an important functional component of JDH and inhibits EMT, and therefore cell migration and invasion.

The Smad3/Smad7 cascade is important for the regulation of EMT

The Smad3/Smad7 cascade is the target of the JDH treatment; it regulates and subsequently inhibits EMT. However, it is still not clear whether the Smad3/Smad7 cascade is directly correlated with EMT. Therefore, we conducted both over-expression and suppression assays of Smad3 and Smad7, respectively, for further verification. The MHCC-97L cell line has low expression levels of Smad3 but high expression levels of Smad7, and was determined to be a better choice for the assays. Depending on the application of the Smad3 overexpression vector, the expression of both Smad3 and p-Smad3 were upregulated (**Figure 6A**). Meanwhile, E-cadherin expression decreased, but N-cadherin and Vimentin showed higher expression levels compared with the control group. The wound closure rate (**Figure 6B** and **6D**) and the number of invasive cells (**Figure 6C** and **6E**) were enhanced significantly, indicating EMT activation. However, this phenomenon was

inhibited by the addition of JHD, which prevented cell migration and invasion.

On the other hand, the Smad7 suppression assay was carried out with Smad7-targeting shRNA, the results of which were consistent with those of the Smad3 overexpression assay. After suppressing Smad7 expression, the E-cadherin level decreased accordingly but the N-cadherin and Vimentin levels increased (**Figure 7A**). The application of shRNA induced a more active cell migration (**Figure 7B**) and invasion (**Figure 7C**). However, both were inhibited after the addition of the drug-serum. An immunofluorescence microscopy assay was carried out in order to determine the level of EMT. According to the results, E-cadherin levels decreased but N-cadherin levels increased with the application of Smad7-targeting shRNA. However, the application of drug-serum enhanced E-cadherin levels and slightly attenuated N-cadherin. This indicates that EMT is inhibited by the drug-serum and that Smad3 and Smad7 are closely correlated with EMT, but the JHD induced drug-serum could inhibit the process and, thus, hepatic carcinomatous cell migration and invasion.

JHD treatment inhibits carcinomatous metastasis in nude mice

In order to verify the in vivo functions of JHD and its potential value in treating hepatic carcinoma, the subcutaneous tumor formation assay was carried out. The results were consistent with the in vitro experiment in SMMC7221 cells; the occurrence rate of liver-metastasis in the mice without JHD treatment was 70%, whereas animals with JHD treatment presented a lower ratio of 40% (**Figure 8A**). The tumorous tissue from both groups was extracted, as described above. The tumors were gray to gray-white in color, presented as soft masses, and consisted of variably size nodules that were usually coalescent. By comparison, both the size and number of tumors from the mice in the control group were larger than those in the JHD treatment group (**Figure 8B**). The tissues were collected for a pathological staining assay and images obtained with microscopy (**Figure 8C**) showed that the average tumor size from the control group was larger than that from the JHD treatment group. Compared with the JHD treatment group, there was more intensive vasculature inside the tumor tissues of the control

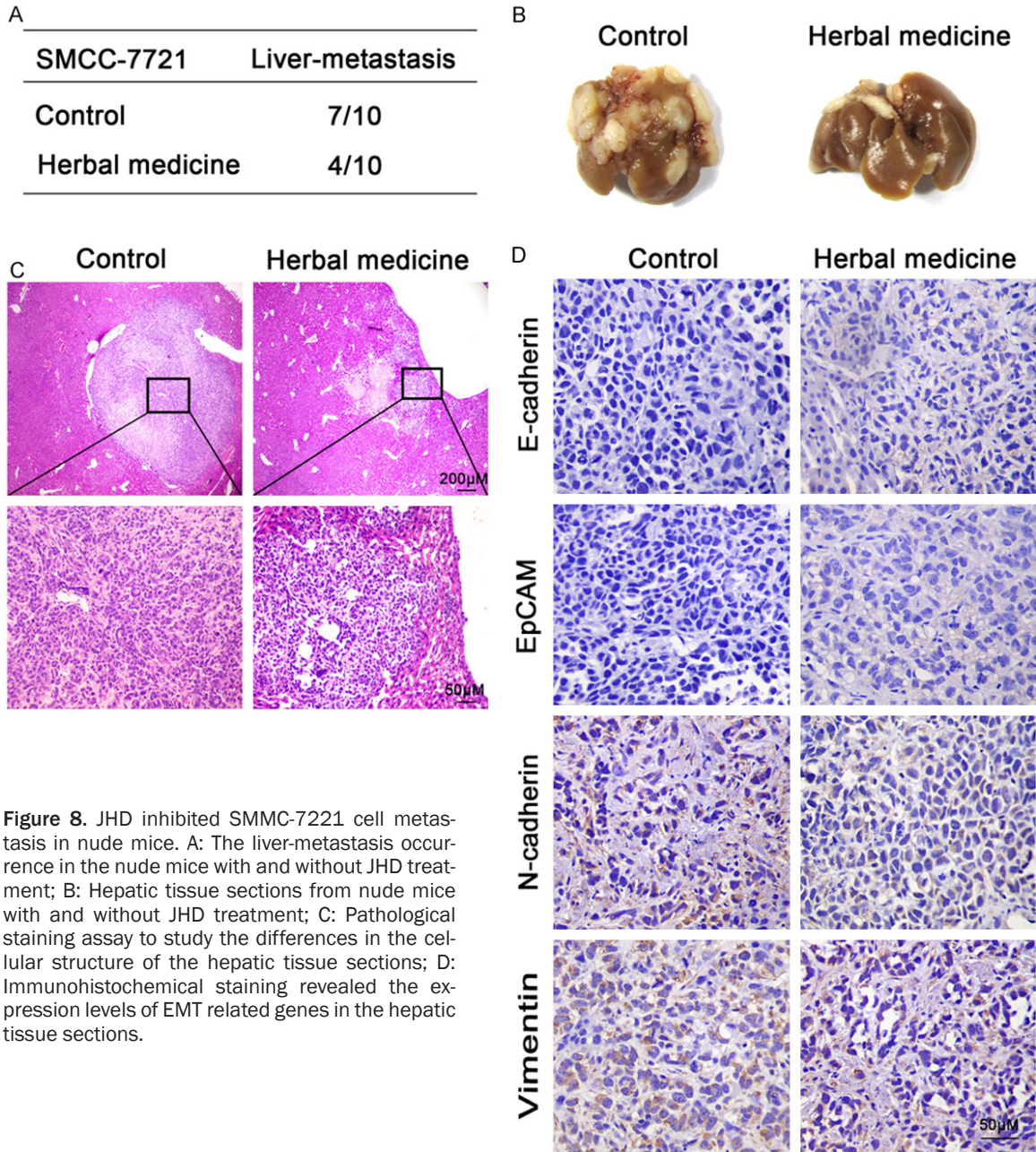


Figure 8. JHD inhibited SMMC-7721 cell metastasis in nude mice. A: The liver-metastasis occurrence in the nude mice with and without JHD treatment; B: Hepatic tissue sections from nude mice with and without JHD treatment; C: Pathological staining assay to study the differences in the cellular structure of the hepatic tissue sections; D: Immunohistochemical staining revealed the expression levels of EMT related genes in the hepatic tissue sections.

group, which were dark in color. In addition, we performed immunohistochemical staining to evaluate the levels of molecules expressed during EMT. The target molecules were stained yellow in this study. According to the images (**Figure 8D**), in the JHD treatment group, the expression levels of E-cadherin and EpCAM were higher than in the control. Both N-cadherin and Vimentin had low expression in the JHD group, while they were significantly highly expressed in the control group. This indicated that the significance of EMT is higher in the con-

trol group without JHD treatment. In other words, the JHD treatment efficiently inhibited EMT and, therefore, prevented oncogenesis and tumor metastasis.

Meanwhile, we carried out a similar assay by injecting MHCC-97L cells to test the effects of both Smad7 and JHD treatments (**Figure 9**). The results were consistent with the in vitro cell experiments. As indicated in the previous results, when MHCC-97L cells are transfected with Sh-Smad7, Smad7 expression significantly

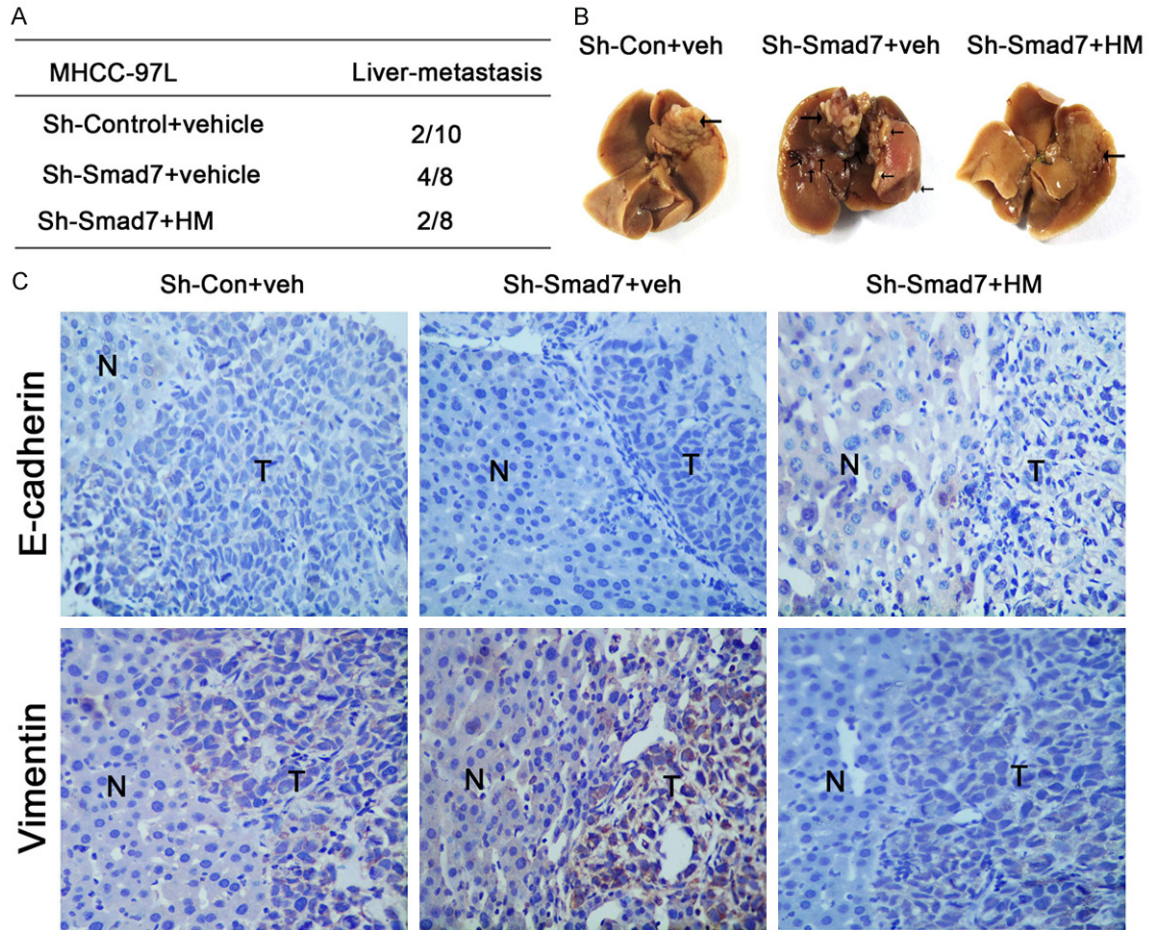


Figure 9. MHCC-97 cell-generated tumor was inhibited from metastasis by JHD. **A:** The liver-metastasis occurrence in the nude mice; **B:** The sections of the hepatic tumor tissues from the nude mice; **C:** Immunohistochemical staining indicated the expression levels of the E-cadherin and Vimentin: "N": tumor-adjacent normal tissue, and "T": tumor tissue, HM: Herbal medicine.

decreases and leads to EMT. Therefore, the percentage of liver-metastasis in mice from the Sh-Smad7+vehicle group reached 50%, which was significantly higher than what was seen in the Sh-Control+vehicle group (**Figure 9A**). The tumorous tissue from the Sh-Smad7+vehicle group presented an even darker color (**Figure 9B**) and a high expression level of Vimentin was detected in both the tumor and tumor-adjacent normal tissue (**Figure 9C**). At this moment, we attempted to use the JHD extract solution to relieve the tumor-metastasis. The efficacy of the herbal medicine was obvious. Compared with the Sh-Smad7+vehicle group, the occurrence of the liver-metastasis in the Sh-Smad7+HM group decreased from 50% to 25% (**Figure 9A**). The shape and pattern of the tumor tissue presented as normal and was not as dark as that of the Sh-Smad7+vehicle group (**Figure**

9B). The expression level of the Vimentin significantly decreased in the Sh-Smad7+HM group compared with the Sh-Smad7+vehicle group (**Figure 9C**). However, the expression level of E-cadherin was not very significantly different among the three groups (**Figure 9C**). This might be due to the feature of MHCC-97L cells to be inactive during tumor metastasis. In general, the above results demonstrate that the suppression of Smad7 led to a higher expression level of Vimentin, thereby leading to tumor metastasis, while JHD treatment decreased the expression level of Vimentin and prevented the tumor from metastasizing.

Discussion

Traditional Chinese medicine has been widely used in China to treat various diseases, including cancer. Chinese medicine has been gaining

increasing attention for its antitumor effects and its comprehensive focus. In this study, we investigated the antitumor functions of JHD and its effect on the proliferation of hepatic cancerous cells and in nude mice.

JHD inhibited the expression of p-Smad3 and enhanced the level of Smad7, therefore inhibiting EMT. EMT is comprised of a series of phenotypic and molecular changes that occur in various steps in cancer cells, like invasion and metastasis [19, 20]. The loss of E-cadherin is the hallmark of EMT. Many factors have been implicated in the transcriptional repression of E-cadherin, including the zinc-finger proteins of the Snail/Slug family, Twist, ZEB1, SIP1, and the basic helix-loop-helix factors. Among these, Snail is one of the most important transcriptional repressors of E-cadherin [21, 22]. Our results are consistent with these previous findings. Without JHD treatment, E-cadherin expression was maintained at low levels, indicating the potential occurrence of EMT. JHD treatment influenced the expressions of both Snail and E-cadherin. By suppressing Snail expression, its inhibitory effects were weakened, allowing E-cadherin to experience increased expression and to prevent EMT. However, Snail was inhibited by JHD when using a high concentration drug-serum (**Figure 1B** and **1F**). Moreover, when using Tan IIA as the drug media, the expression of Snail was not shown to be Tan IIA-concentration dependent (**Figure 3D**). This suggests that Snail is an important factor affecting EMT, but might not be the main target of JHD and Tan IIA in regulating EMT.

At the same time, a TGF- β 1 solution was applied, since emerging evidence suggests that it plays a pivotal role in EMT [23]. Its downstream signaling molecules, including Smad3 and Smad7, have been implicated in TGF- β 1 induced EMT [24, 25]. According to a previous study, TGF- β 1 signaling is activated, which triggers downstream signaling, depending on the mitogen-activated protein kinase (MAPK) pathway [26]. The Smad2/3 cascade is the important factor through which the activation signal is received and then transmitted downstream [27]. According to our results, TGF- β 1 did not change the expression level of Smad3 but only its phosphorylation (**Figure 4A** and **4B**), whereas treatment with JHD blocked this process and inhibited EMT. Thus, JHD is shown to be a signal suppressor of the TGF- β -induced EMT

pathway. However, there might not be a direct correlation between JHD and Smad3, since the expression of Smad7 was shown to increase. Smad7 is an inhibitory factor that blocks the function of Smad3. It interferes with the Smad signaling by preventing the phosphorylation of Smad2/3, which normally occurs following binding of TGF β and activin to their cell surface receptors [28-31]. Recently, the transient introduction of the Smad7 gene using an adenovirus vector has been shown to be effective in treating tissue inflammatory disorders in the lung, kidney, and liver [32-34]. Therefore, increased expression of Smad7 was supposed to prevent EMT. After JHD treatment, Smad7 expression significantly increased and hepatic cell metastasis and invasion were prevented. Therefore, we hypothesize that JHD performs its function mainly through the Smad3/Smad7 cascade by increasing Smad7 expression and inhibiting the phosphorylation of Smad3 via Smad7. Because of this, the TGF- β 1 signaling pathway will eventually be impaired; because of the loss of p-Smad3, the downstream pathway cannot be activated. In addition, this process is independent and distinct from the levels of TGF- β 1, Smad3, and Smad7. According to our results, JHD inhibited EMT with or without TGF- β 1 treatment (**Figure 4**). Although the expressions of Smad3 and Smad7 were adjusted to increase or decrease, respectively, the effect of JHD was almost the same and eventually inhibited EMT (**Figures 6** and **7**). Therefore, JHD showed a predominant anti-tumor effect, which was proven in the nude mice assay (**Figures 8** and **9**).

Tan IIA is an herbal monomer isolated from *Salvia miltiorrhiza*, which has been previously reported to attenuate HCC metastases [35] and Tan IIA exhibits direct vasoactive and certain antitumor properties [36-38]. Since *Salvia miltiorrhiza* is one of the components in the JHD formula, it is possible that Tan IIA might be the only active EMT inhibitor. In fact, the inhibition of EMT by Tan IIA has been discovered in a variety of research. According to these studies, Tan IIA inhibits metastasis and prolongs survival via vascular normalization [39], down-regulation of the HIF-1 α [40], and alteration of the TGF- β 1/Smad pathway [41]. In our study, the effect of Tan IIA on the TGF- β 1/Smad pathway was significant. This was generally consistent with the increase in Smad7 levels attributed to

JHD, decreasing p-Smad3 levels, and eventually suppressing cell invasion and metastasis (Figures 3 and 5). These results were also similar to previous research on renal interstitial fibroblasts in rats [42]. Therefore, Tan IIA might be one of the crucial components of the JHD formula that targets on the TGF- β 1/Smad pathway and attenuates EMT.

From this research and previous studies, traditional Chinese medicine can be understood to hold the potential capacity for treating hepatic carcinoma. We elucidated the function of JHD treatment that inhibits hepatic cancerous cell metastasis and invasion by regulating the Smad3/Smad7 cascade. Therefore, JHD might have applications for the clinical treatment of hepatic carcinoma. However, since the results from this study were based on *in vitro* assays of hepatic cancerous cells and *in vivo* assays in nude mice, clinical data from HCC patients is necessary. Future studies will be focused on clinical assays in the patients treated with JHD. The prognosis data can be used as evidence to suggest the possibility of JHD as a therapy for the treatment of hepatic carcinoma.

Acknowledgements

This study was supported by the National Natural Science Foundation of China (8140-3397), the Natural Science Foundation of Guangdong Province, China (2014A0303134-08), and the Science and Technology Planning Project of Guangdong Province, China (2016-A020226052).

Disclosure of conflict of interest

None.

Address correspondence to: Dr. Chong Zhong, Department of Hepatobiliary Surgery, The First Affiliated Hospital of Guangzhou University of Chinese Medicine, 16 Airport Road, Guangzhou 510405, Guangdong, China. Tel: +86-020-36596301; Fax: +86-020-36591595; E-mail: sumszhong@yahoo.com; Dr. Rong-Ping Guo, Department of Hepatobiliary Surgery, Cancer Center of Sun Yat-sen University, 651 Dongfeng Road East, Guangzhou 510061, China. Tel: +86-020-87343114; Fax: +86-020-365-93585; E-mail: guorongp@mail.sysu.edu.cn

References

[1] Llovet JM, Zucman-Rossi J, Pikarsky E, Sangro B, Schwartz M, Sherman M and Gores G. He-

patocellular carcinoma. *Nat Rev Dis Primers* 2016; 2: 16018.

- [2] Chen W, Zheng R, Baade PD, Zhang S, Zeng H, Bray F, Jemal A, Yu XQ and He J. Cancer statistics in China, 2015. *CA Cancer J Clin* 2016; 66: 115-32.
- [3] European association for the study of the liver; European organisation for research and treatment of cancer. *EASL-EORTC clinical practice guidelines: management of hepatocellular carcinoma. J Hepatol* 2012; 56: 908-943.
- [4] Bruix J, Reig M and Sherman M. Evidence-based diagnosis, staging, and treatment of patients with hepatocellular carcinoma. *Gastroenterology* 2016; 150: 835-853.
- [5] Thiery JP, Acloque H, Huang RY and Nieto MA. Epithelial-mesenchymal transitions in development and disease. *Cell* 2009; 139: 871-890.
- [6] Grille SJ, Bellacosa A, Upson J, Klein-Szanto AJ, van Roy F, Lee-Kwon W, Donowitz M, Tsihchlis PN and Larue L. The protein kinase Akt induces epithelial mesenchymal transition and promotes enhanced motility and invasiveness of squamous cell carcinoma lines. *Cancer Res* 2003; 63: 2172-2178.
- [7] Thompson EW, Newgreen DF and Tarin D. Carcinoma invasion and metastasis: a role for epithelial-mesenchymal transition? *Cancer Res* 2005; 65: 5991-5995; discussion 5995.
- [8] Lim J and Thiery JP. Epithelial-mesenchymal transitions: insights from development. *Development* 2012; 139: 3471-3486.
- [9] Grunert S, Jechlinger M and Beug H. Diverse cellular and molecular mechanisms contribute to epithelial plasticity and metastasis. *Nat Rev Mol Cell Biol* 2003; 4: 657-665.
- [10] Kudo-Saito C, Shirako H, Takeuchi T and Kawakami Y. Cancer metastasis is accelerated through immunosuppression during Snail-induced EMT of cancer cells. *Cancer Cell* 2009; 15: 195-206.
- [11] Nieto MA. The snail superfamily of zinc-finger transcription factors. *Nat Rev Mol Cell Biol* 2002; 3: 155-166.
- [12] Spagnoli FM, Cicchini C, Tripodi M and Weiss MC. Inhibition of MMH (Met murine hepatocyte) cell differentiation by TGF(beta) is abrogated by pre-treatment with the heritable differentiation effector FGF1. *J Cell Sci* 2000; 113: 3639-3647.
- [13] Li Q, Zhou S, Jing J, Yang T, Duan S, Wang Z, Mei Q and Liu L. Oligosaccharide from apple induces apoptosis and cell cycle arrest in HT29 human colon cancer cells. *Int J Biol Macromol* 2013; 57: 245-254.
- [14] Gordaliza M. Natural products as leads to anti-cancer drugs. *Clin Transl Oncol* 2007; 9: 767-776.
- [15] Harvey AL. Natural products in drug discovery. *Drug Discov Today* 2008; 13: 894-901.

Jianpi Huayu Decoction inhibits EMT

- [16] Newman DJ, Cragg GM and Snader KM. The influence of natural products upon drug discovery. *Nat Prod Rep* 2000; 17: 215-234.
- [17] Tian XY and Liu L. Drug discovery enters a new era with multi-target intervention strategy. *Chin J Integr Med* 2012; 18: 539-542.
- [18] Zou X, Wang RP, Li D. Effects serum with Jianpi Huayu prescription on apoptosis of human colon cancer cell Iovo. *Liaoning Journal of Traditional Chinese Medicine* 2011; 38: 2355-2356.
- [19] Heldin CH, Vanlandewijck M and Moustakas A. Regulation of EMT by TGF β in cancer. *FEBS Lett* 2012; 586: 1959-1970.
- [20] Brabletz T. EMT and MET in metastasis: where are the cancer stem cells? *Cancer Cell* 2012; 22: 699-701.
- [21] Barrallo-Gimeno A and Nieto MA. The Snail genes as inducers of cell movement and survival: implications in development and cancer. *Development* 2005; 132: 3151-3161.
- [22] Dong C, Wu Y, Yao J, Wang Y, Yu Y, Rychahou PG, Evers BM and Zhou BP. G9a interacts with Snail and is critical for Snail-mediated E-cadherin repression in human breast cancer. *J Clin Invest* 2012; 122: 1469-1486.
- [23] Bottinger EP. TGF-beta in renal injury and disease. *Semin Nephrol* 2007; 27: 309-320.
- [24] Zhu HJ, Iaria J and Sizeland AM. Smad7 differentially regulates transforming growth factor beta-mediated signaling pathways. *J Biol Chem* 1999; 274: 32258-32264.
- [25] Kavsak P, Rasmussen RK, Causing CG, Bonni S, Zhu H, Thomsen GH and Wrana JL. Smad7 binds to Smurf2 to form an E3 ubiquitin ligase that targets the TGF beta receptor for degradation. *Mol Cell* 2000; 6: 1365-1375.
- [26] Yang YC, Piek E, Zavadil J, Liang D, Xie D, Heyer J, Pavlidis P, Kucherlapati R, Roberts AB and Bottinger EP. Hierarchical model of gene regulation by transforming growth factor beta. *Proc Natl Acad Sci U S A* 2003; 100: 10269-10274.
- [27] Roberts AB, Tian F, Byfield SD, Stuelten C, Ooshima A, Saika S and Flanders KC. Smad3 is key to TGF-beta-mediated epithelial-to-mesenchymal transition, fibrosis, tumor suppression and metastasis. *Cytokine Growth Factor Rev* 2006; 17: 19-27.
- [28] Moustakas A, Pardali K, Gaal A and Heldin CH. Mechanisms of TGF-beta signaling in regulation of cell growth and differentiation. *Immunol Lett* 2002; 82: 85-91.
- [29] Ten Dijke P, Goumans MJ, Itoh F and Itoh S. Regulation of cell proliferation by Smad proteins. *J Cell Physiol* 2002; 191: 1-16.
- [30] Massague J and Wotton D. Transcriptional control by the TGF-beta/Smad signaling system. *EMBO J* 2000; 19: 1745-1754.
- [31] Derynck R and Zhang YE. Smad-dependent and Smad-independent pathways in TGF-beta family signalling. *Nature* 2003; 425: 577-584.
- [32] Nakao A, Fujii M, Matsumura R, Kumano K, Saito Y, Miyazono K and Iwamoto I. Transient gene transfer and expression of Smad7 prevents bleomycin-induced lung fibrosis in mice. *J Clin Invest* 1999; 104: 5-11.
- [33] Lan HY, Mu W, Tomita N, Huang XR, Li JH, Zhu HJ, Morishita R and Johnson RJ. Inhibition of renal fibrosis by gene transfer of inducible Smad7 using ultrasound-microbubble system in rat UUO model. *J Am Soc Nephrol* 2003; 14: 1535-1548.
- [34] Dooley S, Hamzavi J, Breitkopf K, Wiercinska E, Said HM, Lorenzen J, Ten Dijke P and Gressner AM. Smad7 prevents activation of hepatic stellate cells and liver fibrosis in rats. *Gastroenterology* 2003; 125: 178-191.
- [35] Huang XY, Huang ZL, Wang L, Xu YH, Huang XY, Ai KX, Zheng Q and Tang ZY. Herbal compound "Songyou Yin" reinforced the ability of interferon- α to inhibit the enhanced metastatic potential induced by palliative resection of hepatocellular carcinoma in nude mice. *BMC Cancer* 2010; 10: 580.
- [36] Wang J, Dong MQ, Liu ML, Xu DQ, Luo Y, Zhang B, Liu LL, Xu M, Zhao PT, Gao YQ and Li ZC. Tanshinone IIA modulates pulmonary vascular response to agonist and hypoxia primarily via inhibiting Ca $^{2+}$ influx and release in normal and hypoxic pulmonary hypertension rats. *Eur J Pharmacol* 2010; 640: 129-138.
- [37] Fan G, Zhu Y, Guo H, Wang X, Wang H and Gao X. Direct vasorelaxation by a novel phytoestrogen tanshinone IIA is mediated by nongenomic action of estrogen receptor through endothelial nitric oxide synthase activation and calcium mobilization. *J Cardiovasc Pharmacol* 2011; 57: 340-347.
- [38] Wang L, Zhou GB, Liu P, Song JH, Liang Y, Yan XJ, Xu F, Wang BS, Mao JH, Shen ZX, Chen SJ and Chen Z. Dissection of mechanisms of Chinese medicinal formula Realgar-Indigo naturalis as an effective treatment for promyelocytic leukemia. *Proc Natl Acad Sci U S A* 2008; 105: 4826-4831.
- [39] Wang WQ, Liu L, Sun HC, Fu YL, Xu HX, Chai ZT, Zhang QB, Kong LQ, Zhu XD, Lu L, Ren ZG and Tang ZY. Tanshinone IIA inhibits metastasis after palliative resection of hepatocellular carcinoma and prolongs survival in part via vascular normalization. *J Hematol Oncol* 2012; 5: 69.
- [40] Fu P, Du F, Chen W, Yao M, Lv K and Liu Y. Tanshinone IIA blocks epithelial-mesenchymal transition through HIF-1 α downregulation, reversing hypoxia-induced chemotherapy re-

Jianpi Huayu Decoction inhibits EMT

- sistance in breast cancer cell lines. *Oncol Rep* 2014; 31: 2561-2568.
- [41] Wang DT, Huang RH, Cheng X, Zhang ZH, Yang YJ and Lin X. Tanshinone IIA attenuates renal fibrosis and inflammation via altering expression of TGF-beta/Smad and NF-kappaB signaling pathway in 5/6 nephrectomized rats. *Int Immunopharmacol* 2015; 26: 4-12.
- [42] Tang J, Zhan C and Zhou J. Effects of tanshinone IIA on transforming growth factor beta1-Smads signal pathway in renal interstitial fibroblasts of rats. *J Huazhong Univ Sci Technolog Med Sci* 2008; 28: 539-542.